We are IntechOpen, the world's leading publisher of Open Access books
Built by scientists, for scientists

4,800
Open access books available

122,000
International authors and editors

135M
Downloads

Our authors are among the

154
Countries delivered to

TOP 1%
most cited scientists

12.2%
Contributors from top 500 universities

CLARIVATE ANALYTICS
BOOK CITATION INDEX
INDEXED

WEB OF SCIENCE™

Selection of our books indexed in the Book Citation Index in Web of Science™ Core Collection (BKCI)

Interested in publishing with us?
Contact book.department@intechopen.com

Numbers displayed above are based on latest data collected.
For more information visit www.intechopen.com

Chapter 3

Prefabricated Steel-Reinforced Concrete Composite Column

Hyeon-Jong Hwang

Additional information is available at the end of the chapter

http://dx.doi.org/10.5772/intechopen.77166

Abstract

In conventional concrete-encased steel composite columns, a steel section is placed at the center of the cross section. Thus, the contribution of the steel section to the overall flexural capacity of the column could be limited. For better efficiency and economy, particularly under biaxial moment, the steel section needs to be placed at the corners, rather than at the center of the cross section. Recently, a prefabricated steel-reinforced concrete column has been developed to utilize the advantages of the reinforced concrete column and the steel-concrete composite column. In the composite column, four steel angles are placed at the corners of the cross section, and transverse bars and plates are used to connect the angles by welding or bolting. The composite column has been widely applied to industrial buildings that require large sized columns and fast construction. In this chapter, the newly developed composite column is introduced, and basic mechanism, structural performance, and field application case are discussed.

Keywords: metal and composite structures, composite column, steel angle, weld connection, bolt connection, compression test, flexural test, cyclic test

1. Introduction

Nowadays, the demand for huge buildings, long-span structures, and skyscrapers has increased. As a result, (1) sectional performance of compressive members, and (2) fast and safe construction method become important. **Figure 1(a)** shows a conventional concrete-encased steel (CES) composite column using a wide-flange steel section at the center of the cross section. Generally, the wide-flange steel is placed at the center of the cross section, and then longitudinal bars and tie bars are placed in construction site. Thus, the contribution of the steel

IntechOpen

© 2018 The Author(s). Licensee IntechOpen. This chapter is distributed under the terms of the Creative Commons Attribution License (http://creativecommons.org/licenses/by/3.0), which permits unrestricted use, distribution, and reproduction in any medium, provided the original work is properly cited. CC BY

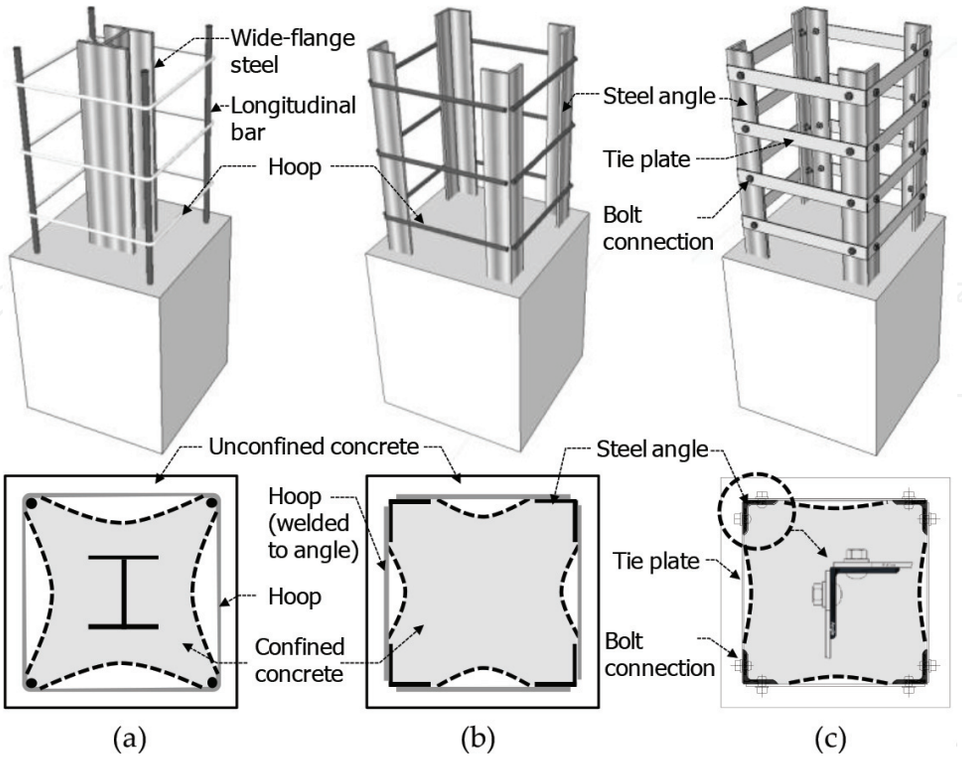

Figure 1. Comparison of CES column and PSRC columns. (a) CES composite column, (b) PSRC composite column (weld connection), (c) PSRC composite column (bolt connection)

section to the overall flexural capacity of the column could be limited. Further, the need for rebar and formwork construction requires considerable construction time. Particularly, in mega structures such as semiconductor factory and warehouse using long and large sized columns, fast and safe construction methods are necessary.

In order to improve structural capacity and cost efficiency, a prefabricated steel-reinforced concrete (PSRC) composite column has been used. As shown in **Figure 1(b)** and **(c)**, the prefabricated steel angles at the four corners replace the conventional wide-flange steel, and the steel angles are weld connected or bolt connected with transverse bars or plates [1–5]. The weld connection should follow the details prescribed in welding standards [6, 7]. The steel angles resist axial load and flexural moment. The transverse bars and plates provide shear resistance, concrete confinement, and bond resistance between the steel angles and concrete. Because the steel cage of angles and transverse reinforcement are prefabricated off site, field rebar work is unnecessary. Further, the self-erectable steel cage can provide sufficient strength and rigidity to support the construction loads of beams and slabs that are superimposed on the PSRC composite column.

Figures 2 and **3** show field application of weld-connected and bolt-connected PSRC composite columns, respectively. Generally, the PSRC composite column with 20 m height and 1.5 m $\times$ 1.5 m to 2.0 m $\times$ 2.0 m sectional area is used for two- or three-story construction at the same time. In the case of the weld-connected PSRC composite column, the steel cage of angles and transverse reinforcement is moved to construction site, and then concrete form is installed (**Figure 2**). On the other hand, in the case of the bolt-connected PSRC composite column,

http://dx.doi.org/10.5772/intechopen.77166

Figure 2. Semiconductor FAB (weld-connected PSRC composite column).

Figure 3. Semiconductor FAB (bolt-connected PSRC composite column).

concrete form is preattached to the steel cage and it can be permanently used after concrete pouring (**Figure 3**). Thus, field work related to reinforcing bar placement and concrete form work is excluded, which improves the construction safety and saves the construction time at working in high place.

2. Structural performance of PSRC column

2.1. Contribution of transverse reinforcement

The prefabricated steel angle composite columns strongly depend on the transverse reinforcement that connects the corner steel angles. The transverse reinforcement provides (1) shear transfer between the steel angles, (2) bond between the steel angles and concrete, (3) buckling resistance for the steel angles, and (4) lateral confinement for the core concrete. To satisfy the requirements of (3) and (4), close spacing as well as sufficient strength are required for the

transverse reinforcement. However, the transverse bars welded to steel angles or the transverse plates bolt-connected to steel angles may cause premature tensile fracture of the connection, which should be considered in design.

Cover concrete provides local buckling resistance and fire resistance for the steel angles. However, when the transverse bars are not closely spaced, the PSRC composite columns are vulnerable to premature spalling of the cover concrete due to smooth surface of steel angles. Particularly, when the columns are subjected to high axial compression force, the load-carrying capacity and deformation capacity of the PSRC composite columns can be degraded by early spalling of the cover concrete. Further, under cyclic lateral loading, the PSRC composite columns are expected to be more susceptible to such damages as the ductility demand increases.

2.2. Compressive strength

2.2.1. Design method

The nominal compressive strengths P_n of a PSRC composite column under concentric axial loading can be evaluated by current design code equations for a concrete-encased steel composite column. For example, AISC 360–10 [8] specifies the nominal compressive strength based on plastic stress and column length effect.

$$P_n = P_{no} \cdot 0.658^{(P_0/P_e)} \tag{1}$$

$$P_{no} = 0.85f'_c\left(A_g - A_s - A_{sr}\right) + F_y A_s + f_{yr}A_{sr} \tag{2}$$

$$P_e = \pi^2\left(EI_{eff}\right)/(KL)^2 \tag{3}$$

$$EI_{eff} = E_s I_s + 0.5E_s I_{sr} + C_1 E_c I_c \tag{4}$$

$$C_1 = 0.1 + 2A_s/(A_c + A_s) \leq 0.3 \tag{5}$$

where P_{no} = maximum compressive strength of the composite column; P_e = elastic buckling strength of the column; f_c' = concrete strength; F_y and A_s = yield strength and area of the steel section, respectively; f_{yr} and A_{sr} = yield strength and area of the longitudinal bars, respectively; EI_{eff} = effective flexural stiffness of the composite column; KL = effective buckling length; E_s = elastic modulus of steel; E_c = elastic modulus of concrete (= $4700\sqrt{f_c'}$); I_s, I_{sr}, and I_c = second-order moments of inertia of the steel section, reinforcing bar, and concrete, respectively, with respect to the centroid of the column section; and A_c = concrete area.

For better evaluation of the load-carrying capacity of a PSRC composite column, numerical analysis using the stress–strain relationship of confined concrete, unconfined concrete, and steel can be used as shown in **Figure 4** [1, 3]. The numerical analysis can be performed using strain compatibility method [9]. The stress–strain relationship of confined and unconfined concrete can be determined from various existing models [10–12].

The nominal compressive strengths P_n of a PSRC composite column under eccentric axial loading can be evaluated by assuming plastic stress distribution of the composite section. In

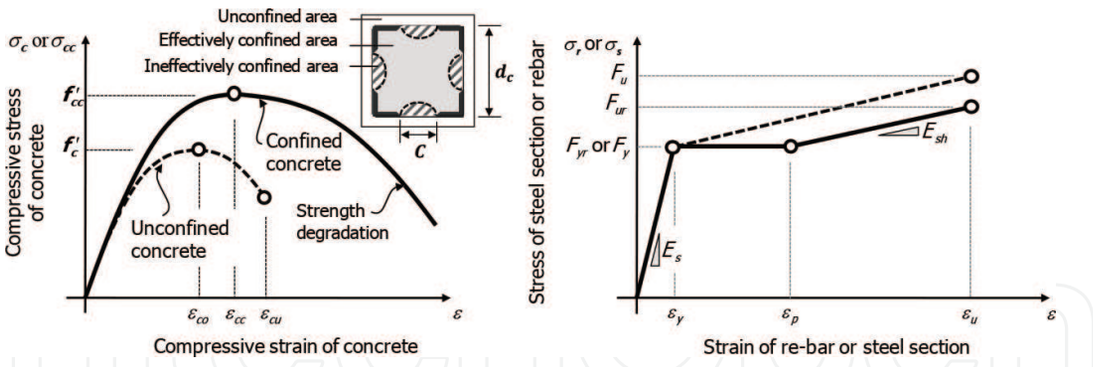

Figure 4. Stress–strain relationships of concrete and steel for numerical analysis.

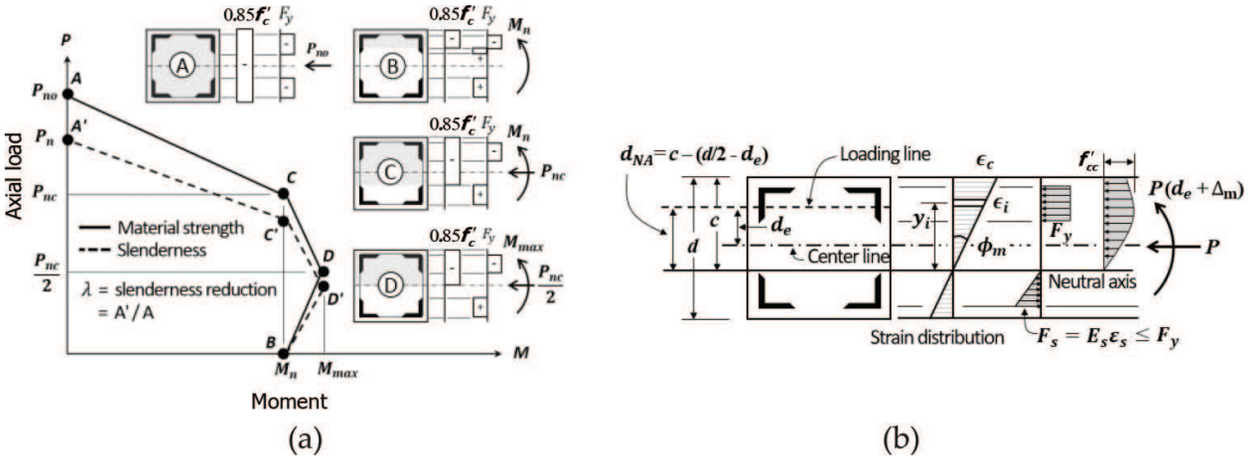

Figure 5. Section analysis methods of PSRC column under eccentric axial loading: (a) *P-M* interaction diagram and (b) strain-compatibility method.

Figure 5(a), performance points A and B indicate pure compressive strength P_{no} and moment strength M_n, respectively. Performance points C indicates the compressive strength P_{nc} corresponding to the moment M_n. Performance points D indicates the maximum moment strength corresponding to $P_{nc}/2$. Considering the slenderness effect of columns, each performance point should be decreased by multiplying the slenderness reduction factor λ to the compressive strength (where λ = ratio of P_n to P_{no}). Further, using the strain-compatibility method, *P-M* interaction diagram can be estimated (**Figure 5(b)**).

2.2.2. Structural test

Figure 6 shows the test setup for the concentric axial loading and eccentric axial loading tests. The eccentricity can be controlled using the distance between the column center and loading center. During the test, the load-carrying capacity, axial shortening, and horizontal expansion were measured to evaluate the structural performance of the PSRC composite columns.

Figure 7(a) compares the axial load-strain relationships of a CES and PSRC composite columns using steel ratio of 2.0% under concentric axial compression force [3–5]. The axial load behavior of the PSRC composite column was similar to that of the CES composite column. The

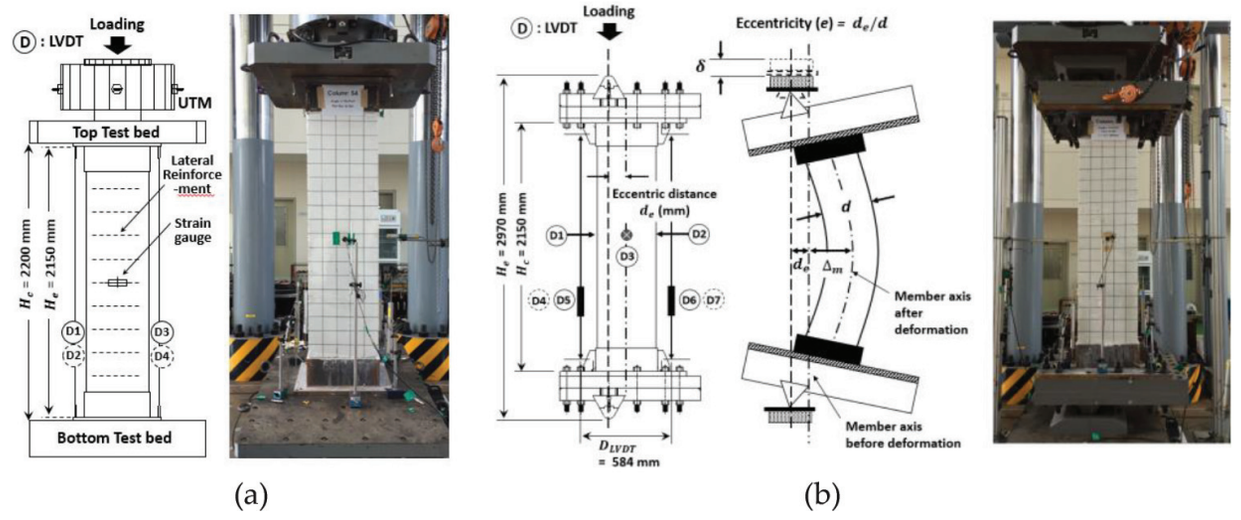

Figure 6. Test setup of compressive loading tests: (a) concentric axial loading and (b) eccentric axial loading.

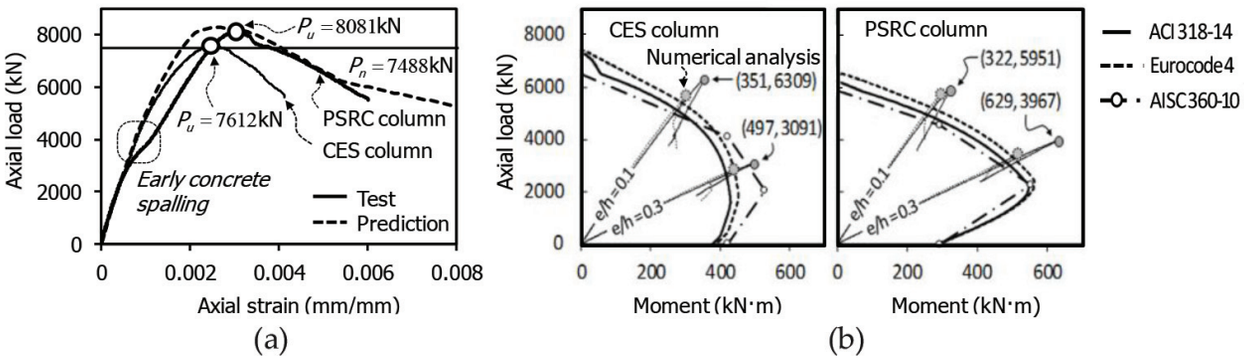

Figure 7. Axial load-carrying capacities of CES and PSRC columns: (a) concentric axial loading and (b) eccentric axial loading.

contribution of the steel angles to the lateral confinement increased the peak strength P_u and the deformation capacity in the PSRC composite column. Under concentric axial force, local buckling of the steel angles was not observed. After the peak strengths, significant cracking and subsequent concrete spalling occurred. Particularly, the early spalling can be initiated at the corners of the cross section because of the smooth surface of the angle. Thus, to secure robust axial load behavior of the PSRC composite columns under high axial load, it is recommended that the spacing of transverse reinforcement be decreased to half of the requirement of CES composite columns.

Figure 7(b) compares the *P-M* interaction curves of design codes [8, 13, 14] with the test results of CES and PSRC composite columns under eccentric load with a low eccentricity ratio of e/h = 0.1 and 0.3. As the eccentricity ratio increased, the structural behavior changed from compression to flexure. The peak strength of the CES composite column was less than that of the PSRC composite column with e/h = 0.3. This is because the effective compressive area of the steel and concrete sections was increased in the PSRC composite column with large eccentricity. In the PSRC

composite columns, the *P-M* interaction curves of design codes were similarly predicted at the load level of $0.2P_n$ to $0.5P_n$, regardless of the assumption for the stress distribution. Further, the maximum flexural strength predictions of the PSRC composite columns were greater than those of the CES composite columns, because of the steel angles placed at the four corners of the column. This result indicates that when the same amount of the steel is used for composite columns, the flexural strength of PSRC composite columns can be greater than that of CES composite columns under general design compression load (= $0.2P_n$ ~ $0.5P_n$).

2.3. Flexural strength

2.3.1. Flexural design method

The ultimate flexural strength of a PSRC composite column can be evaluated by performing a section analysis based on either plastic stresses (i.e., plastic stress method) or strain-induced stresses (i.e., strain-compatibility method); the stresses of the steel angles, reinforcing bars, and concrete are determined by linear strain distribution and the stress–strain relationships of the materials [1]. **Figure 8** shows the stress distributions at the PSRC cross section by two methods. For the plastic stress method (**Figure 8(a)**), plastic stresses of concrete, steel angles, and reinforcing bars can be used as $0.85f_c'$, F_y, and F_{yr}, respectively. For the strain-compatibility method (**Figure 8(b)**), strain-induced stresses of angles, reinforcing bars, and concrete can be determined assuming linear distribution of strain over the entire cross section.

$$-F_y \le \sigma_s = E_s\varepsilon \le F_y \tag{6}$$

$$-F_{yr} \le \sigma_r = E_s\varepsilon \le F_{yr} \tag{7}$$

$$\sigma_c = f_c'\left(\frac{2\varepsilon}{\varepsilon_{co}} + \left(\frac{\varepsilon}{\varepsilon_{co}}\right)^2\right) \; for - \varepsilon_{cu} \le \varepsilon \le 0 \tag{8}$$

where σ_s, σ_r, σ_c = strain-induced stresses of angles, re-bars, and concrete, respectively; ε = strain which is linearly proportional to the distance from the neutral axis; ε_{co} = strain corresponding to the concrete strength f_c'; and ε_{cu} = ultimate strain of concrete. In σ_s, σ_r, σ_c, and ε, compressive stress and strain are negative values. Perfect bond (or full composite action) between steel

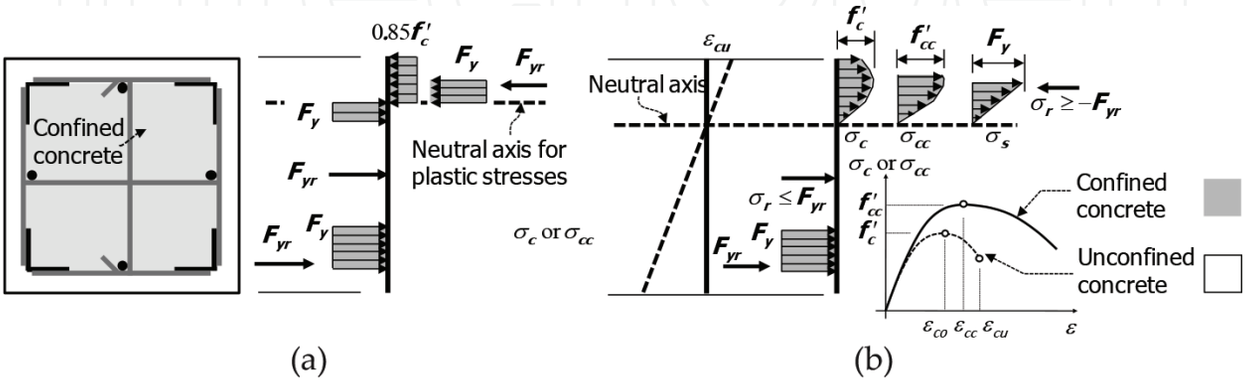

Figure 8. Section analysis methods of PSRC column: (a) plastic stress method and (b) strain-compatibility method.

angles and concrete is assumed for the section analysis. For confined concrete, the stress–strain relationship of the confined concrete can be used.

2.3.2. Shear design method

The shear resistance of a PSRC composite column is provided by concrete, transverse reinforcement, and steel angles. Since the dimensions of the angle cross section are significantly less than that of the entire cross section, the contribution of the angles to the shear strength is neglected. Thus, the nominal shear strength V_n of a PSRC composite column can be calculated, on the basis of current RC design code [13].

$$V_n = \frac{1}{6}\sqrt{f'_c}bd + A_{st}F_{yt}\frac{d}{s} \le \frac{5}{6}\sqrt{f'_c}bd \tag{9}$$

where b = width of the cross section; d = effective depth of the cross section; and A_{st}, F_{yt}, and s = area, yield stress, and spacing of the transverse reinforcement, respectively.

2.3.3. Bond strength design method

Figure 9 shows the details of the weld- or bolt-connection between the steel angles and transverse reinforcement. Before spalling of concrete cover, the shear transfer between the steel angles and concrete is provided by friction of the angle surface and concrete bearing of the transverse reinforcement projected from the angle surface. Conservatively neglecting the frictional resistance, the nominal bond strength B_n of a steel angle is provided by the concrete bearing of the transverse reinforcement [1].

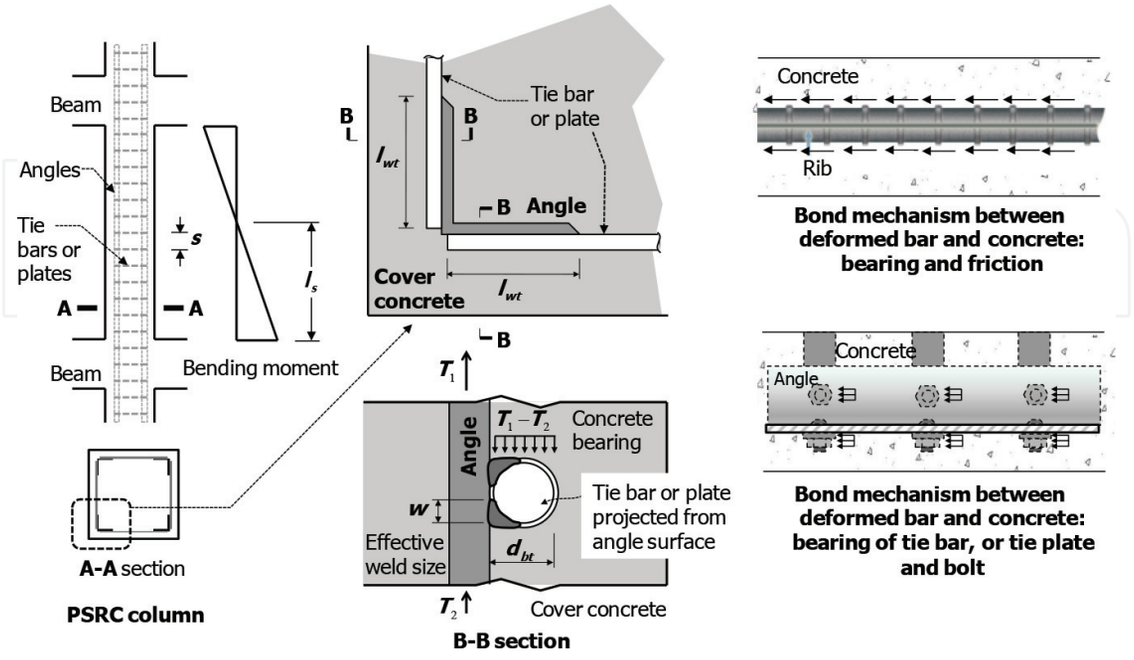

Figure 9. Bond strength between steel angle and concrete.

$$B_n = \alpha\left[0.85f'_c(2d_{bt}l_{wt})\right]\left(\frac{l_s}{s}\right) \tag{10}$$

where d_{bt} = diameter or thickness of a transverse reinforcement projected from the angle surface; l_{wt} = weld length of a transverse bar or projected length of a transverse plate from the angle surface; l_s = shear span length of the PSRC composite column; and α = a factor addressing the confinement effect on the bearing area (≤2.0). After spalling of concrete cover at large inelastic flexural deformation, concrete bearing disappears and is replaced by dowel action of the transverse reinforcement.

2.3.4. Structural test

Figure 10 shows the test setup for the flexural loading tests to investigate the flexural and shear strengths, shear transfer between steel angle and concrete, and strength at the joint between steel angle and transverse reinforcement. The columns are simply supported, and two-point loading is applied at the center of the columns. To estimate the curvature, deflections at least three points need to be measured.

Figure 11(a) shows the moment-curvature relationships at the center span of a CES column and a PSRC column with a cross section of 500 mm × 500 mm (i.e., 2.0% steel ratio) [1]. In the PSRC column using the same steel ratio of the CES column, the peak strength was 56.7% greater than that of the CES column for the following reasons: (1) the yield strength of the steel angles used for the PSRC column was 15.9% greater than that of the wide-flange steel section used for the CES column and (2) the angles placed at the four corners of the cross section can develop 35.2% higher nominal flexural capacity than the center wide-flange steel section. In the PSRC column, the load-carrying capacity was suddenly decreased when bond failure (i.e., concrete bearing failure) occurred in the bottom angles in the shear span (**Figure 12(b)**). After the bond failure, dowel action of the transverse bars developed, causing significant bond-slip deformation. Ultimately, it failed due to the fracture of the transverse bars and spalling of web concrete, which was the typical bond-shear failure mode of the PSRC composite column.

Figure 11(b) compares the effect of transverse reinforcement spacing on the moment-curvature relationship of PSRC composite columns with a smaller cross section of 400 mm × 400 mm

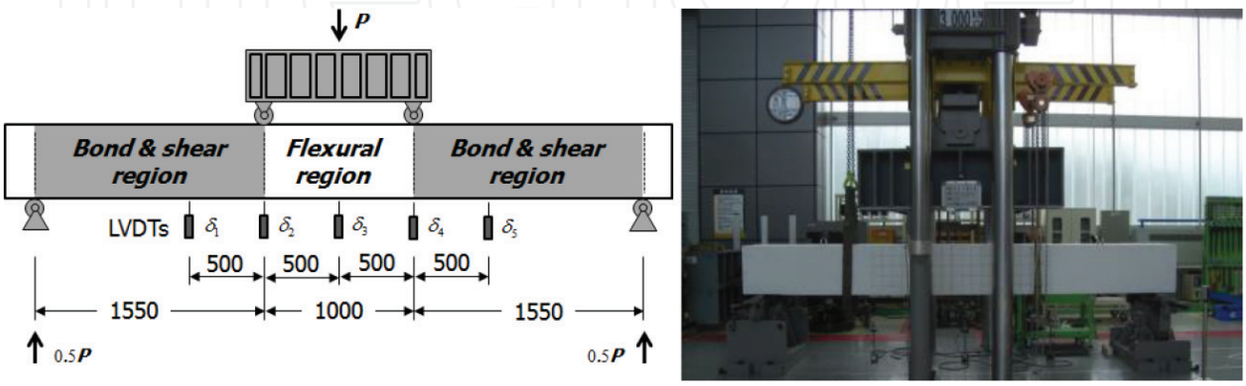

Figure 10. Test setup of flexural loading tests.

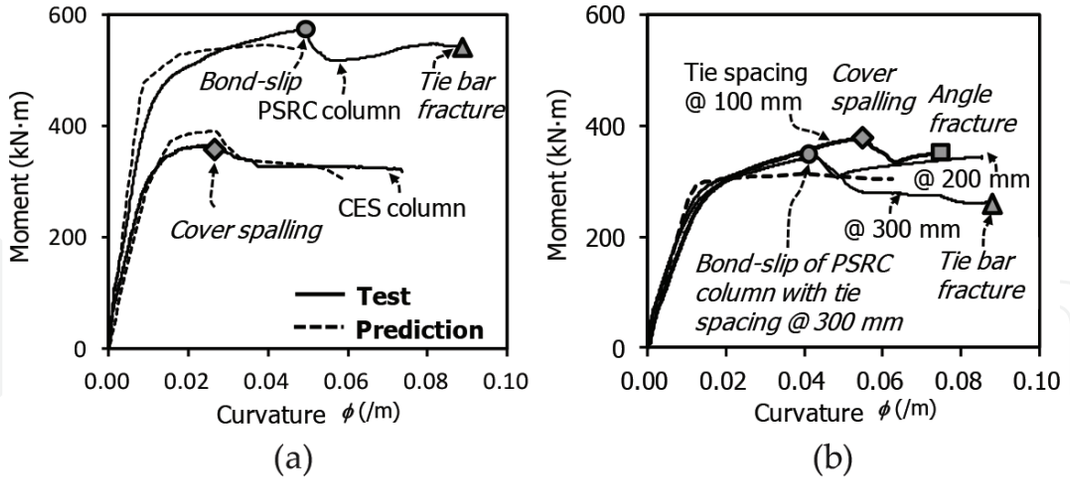

Figure 11. Moment-curvature relationships at the center span of CES and PSRC columns: (a) CES and PSRC columns; (b) PSRC columns according to transverse bar spacing.

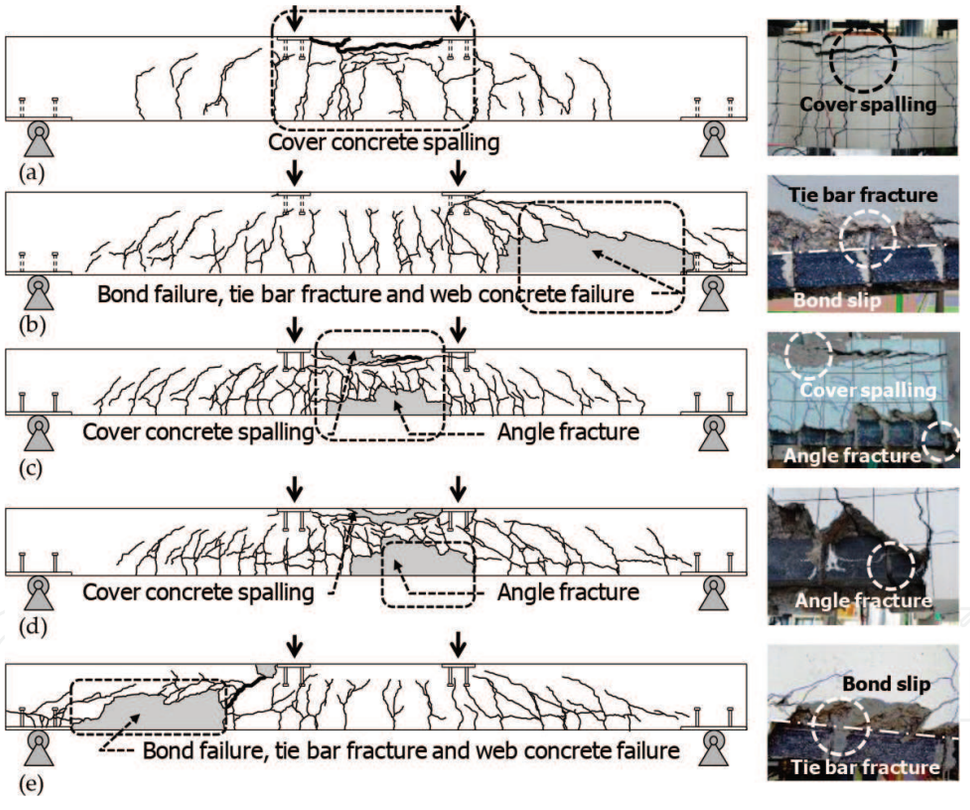

Figure 12. Failure modes of CES and PSRC columns. (a) CES column, (b) PSRC column, (c) PSRC column @ 100 mm tie, (d) PSRC column @ 200 mm tie, (e) PSRC column @ 300 mm tie

(i.e., 3.1% steel ratio). When the transverse reinforcement at a spacing of 100 mm was used, the load-carrying capacity was degraded due to spalling of cover concrete in the uniform moment span, but was slightly recovered due to the strain hardening of the steel angles. Ultimately, it failed due to the tensile fracture of the bottom angle in the uniform moment span (**Figure 12(c)**).

The moment-curvature relationship and failure mode of the PSRC composite column with greater transverse reinforcement spacing of 200 mm were similar to those of the PSRC composite column with transverse reinforcement spacing of 100 mm. It failed due to tensile fracture of the angles in the uniform moment span (**Figure 12(d)**). In the PSRC composite column with the greatest transverse reinforcement spacing of 300 mm, bond failure occurred in the bottom angles. After the bond failure, the load-carrying capacity was significantly decreased due to spalling of web concrete caused by dowel action of the transverse reinforcement. Ultimately, it failed due to fracture of the transverse reinforcement (**Figure 12(e)**).

2.4. Seismic performance

Figure 13 shows the test setup of cyclic loading tests for CES and PSRC composite columns. Using two oil jacks, a uniform axial load corresponding to about 22% of compressive capacity are applied, and a cyclic lateral load is applied using an actuator to the column.

Figure 14 compares the cyclic behaviors of the CES and PSRC composite columns using steel ratio of 2.2%. In the CES composite column, the load-carrying capacity gradually decreased after the peak strength. Although spalling of the cover concrete occurred at the lateral drift of 3.0–4.0% in the plastic hinge region, the load-carrying capacity was not significantly decreased. However, after the spalling of the cover concrete, post-yield buckling occurred in the longitudinal bars. Ultimately, it failed at the drift ratio of 7.0% because of a low cycle fatigue fracture of the longitudinal bars. In the PSRC composite column, the peak strength was 20% greater than that of the CES composite column because of the higher yield strength and the location of the steel angles. Spalling of the cover concrete occurred at the drift ratio of 3.0%, and significant shear cracks occurred in the plastic hinge region because of the increased shear demand. The angles and transverse reinforcement were exposed because of the spalling of cover concrete at the drift ratio of 5.0%. The exposed angles and longitudinal bars were subjected to local

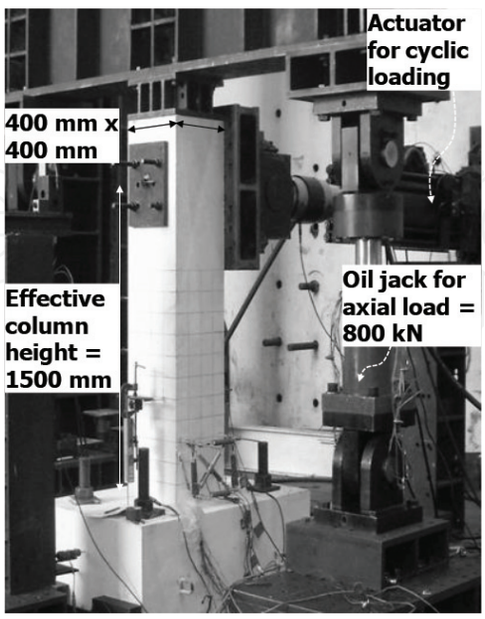

Figure 13. Test setup of cyclic loading tests.

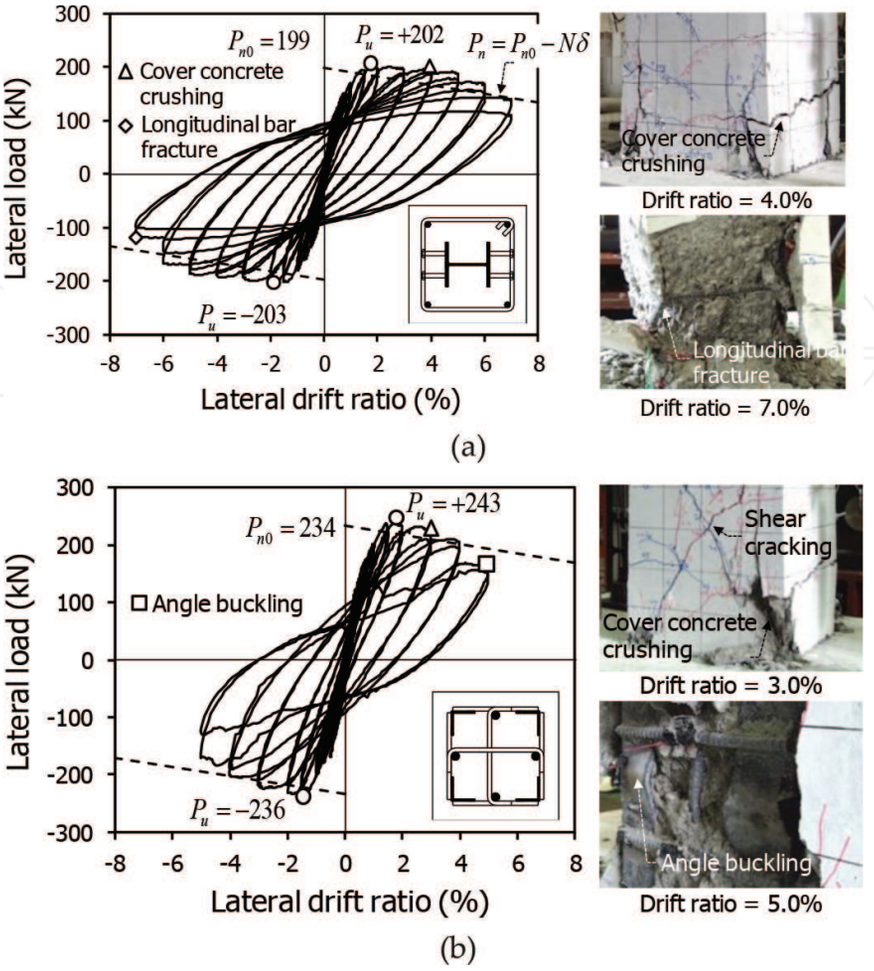

Figure 14. Lateral load-drift relationships of CES and PSRC columns: (a) CES column and (b) PSRC column.

buckling during repeated cyclic loading. As a result, the load-carrying capacity was degraded. However, despite the local buckling of angles and longitudinal bars, tensile fracture did not occur at the joint between the angles and transverse reinforcement.

2.5. Beam-column joint

2.5.1. Design method

Figure 15 shows a U-shaped composite beam-PSRC composite column connection. In order to minimize the workability problem during concrete pouring, only the web plate of the U-section is passed through the joint, and the top and bottom flanges are connected to the top and bottom band plates in the joint. Under high axial compressive force and cyclic lateral loading, premature cover concrete spalling of the joint may deteriorate the connection's strength and deformation capacity.

Figure 16 shows the three mechanisms that contribute to the joint shear strength: web shear yielding of the U-shaped steel section (**Figure 16(a)**), direct strut action of the in-filled concrete

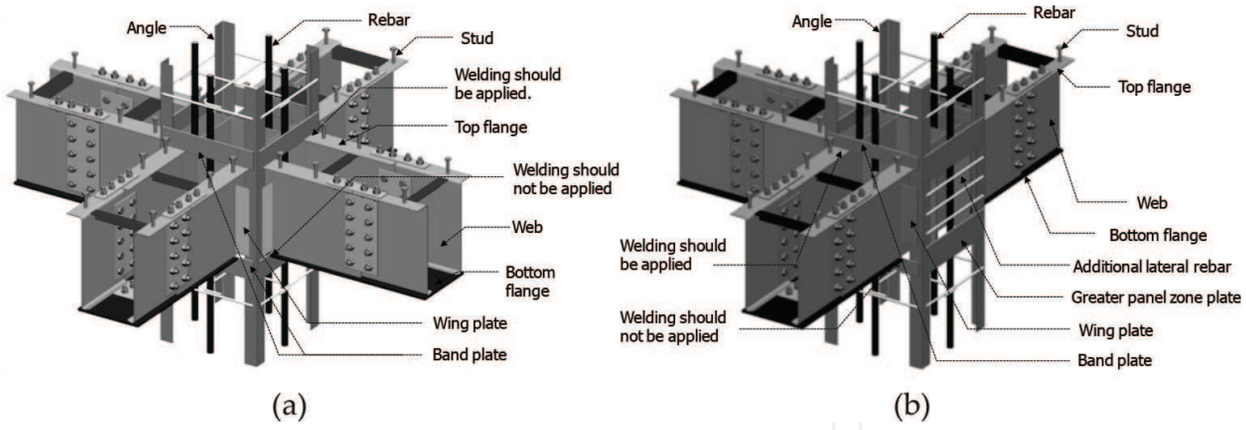

Figure 15. Beam-column joint details: (a) interior beam-column joint and (b) exterior beam-column joint.

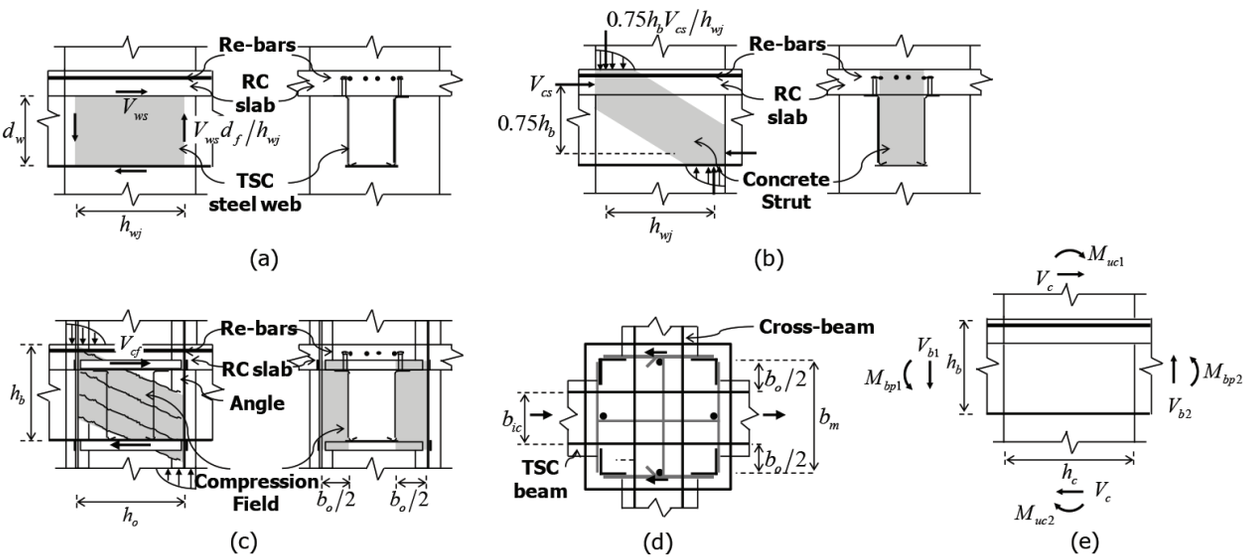

Figure 16. Joint shear strength mechanisms. (a) Web shear yielding (V_{ws}), (b) Concrete diagonal strut (V_{cs}), (c) Strut and tie action (V_{st}), (d) Effective width b_o for interior joint, (e) Joint shear demand.

inside the U-shaped section (**Figure 16(b)**), and the strut-and-tie action between the concrete (outside of the U-shaped section) and the band plates (**Figure 16(c)**) [2]. The shear strength V_{ws} of the two web plates is defined as follows:

$$V_{ws} = (2) \cdot 0.6 F_y t_w h_{wj} \tag{11}$$

where t_w = web thickness; and h_{wj} = effective horizontal length of the web in the joint in the direction of the shear.

The shear strength V_{cs} of the direct concrete strut is defined as follows:

$$V_{cs} = 1.7\sqrt{f'_c}\, b_{ic} h_c \le 0.5 f'_c b_{ic} h_b \quad \text{for the interior joint} \tag{12}$$

$$V_{cs} = 1.2\sqrt{f'_c}\, b_{ic} h_c \le 0.5 f'_c b_{ic} h_b \quad \text{for the exterior joint} \tag{13}$$

where b_{ic} = width of the in-filled concrete, h_c = depth of the PSRC composite column; and h_b = overall depth of the composite beam including the concrete slab.

The shear strength V_{st} of the strut-and-tie action is defined as follows:

$$V_{st} = 0.4\sqrt{f'_c}\, b_o h_o \tag{14}$$

$$b_o = b_{af} - b_{ic} - 2t_w \tag{15}$$

where b_o = effective width of the joint concrete; h_o = effective length of the joint concrete in the direction of shear; b_{af} = distance between the corner angles in the direction orthogonal to the shear; and b_{ic} and t_w = width of the in-filled concrete and web of the U-shaped section, respectively.

For the strut-and-tie mechanism in Eq. (14), the tension force caused by the concrete strut should be resisted by the top and bottom band plates. Thus, the required cross-sectional area A_{bp} of each band plate is calculated as follows:

$$A_{bp} \geq \frac{V_{st}}{2F_{ybp}} \tag{16}$$

where $2F_{ybp}$ = yield strength of the top and bottom band plates.

The joint shear capacity and demand can be expressed as moments, from the static moment equilibrium at the joint (**Figure 16(e)**).

$$\sum M_{uc} - \sum V_b h_o/2 \leq \phi M_{nc} \tag{17}$$

$$\sum M_{uc} = \sum M_{bp} + \sum V_b h_c/2 - V_c h_b \tag{18}$$

$$M_{nc} = V_{ws} d_w + V_{cs}(0.75h_b) + V_{st} d_b \tag{19}$$

where (ΣM_{uc} - ΣV_b h_o/2) and M_{nc} = joint shear demand and capacity, respectively; ΣM_{pb} and ΣV_b = sums of the plastic moments and shear demands, respectively, of the composite beams framing into the joint; V_c = column shear demand; d_w = center-to-center distance between the top and bottom flanges; $0.75h_b$ = approximate moment arm for the composite beam section; and d_b = center-to-center distance between the top and bottom band plates.

2.5.2. Structural test

Figure 17 shows the cyclic lateral load-story drift ratio relationships of U-shaped steel composite beam-PSRC composite column joints. The composite beam has 330 mm width and 700 mm height including slab. The PSRC composite column has 800 mm × 800 mm cross-sectional area. In the interior beam-column joint, cover concrete spalling in the PSRC composite column occurred in the vicinity of the U-section, whose web plate buckled, and severe diagonal cracking occurred in the joint face. The fracture was initiated at the weld joint between the web and the bottom flange and then propagated vertically. Because the band

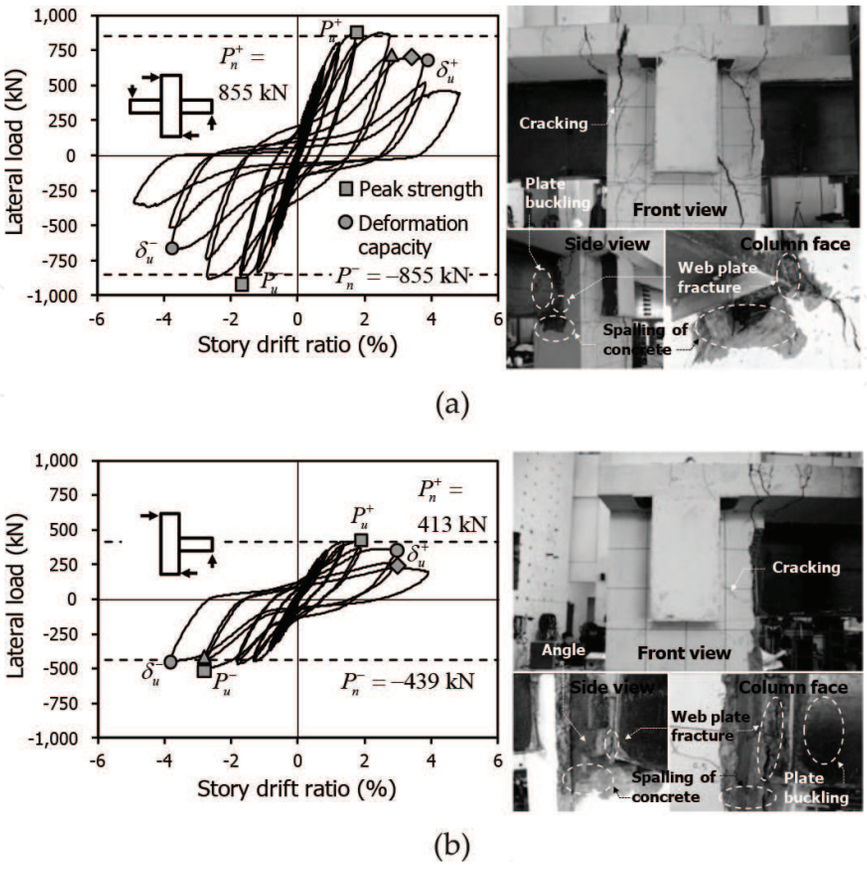

Figure 17. Lateral load-drift relationships: (a) interior beam-column joint and (b) exterior beam-column joint.

plates were not connected to the bottom flange of the U-section, the band plates were not damaged even after cover concrete spalling. However, a gap occurred between the end of the U-section and the column face under positive moments, which was attributed to an anchorage slip of the web plates showing plastic strains inside the joint. As the anchorage slip increased, development of the beam's flexural capacities was delayed, which caused significant pinching in the cyclic behavior. The top band plates welded to the top flange of the U-section were pulled out under a negative moment. In the exterior beam-column joint, after the peak strengths, the load-carrying capacity was significantly degraded because of cover concrete spalling in the PSRC composite column and because of local buckling and fracture of the web in the composite beam. The steel angles of the column were completely exposed.

3. Conclusions

In this chapter, a prefabricated steel-reinforced concrete (PSRC) composite column using steel angles was introduced. Using current design codes, the structural capacities of PSRC composite columns can be evaluated, and it shows better performance than those of a conventional concrete-encased steel (CES) composite column.

- The axial load-carrying capacity and deformation capacity of PSRC composite columns are comparable to, or even better than, those of conventional CES composite columns. In the PSRC composite column under axial compression, the corner angles and the transverse reinforcement provide adequate lateral confinement to the concrete.
- The corner angles of the PSRC composite column increase the flexural strength and stiffness up to about 30%, compared to those of the conventional CES composite columns.
- The bond strength between steel angles and concrete is generated by the bearing strength of the transverse reinforcement projected from the steel angle surface. When the bond strength is greater than the demand (i.e., when close spacing of tie bars is used), the PSRC composite columns show ductile behavior after flexural yielding without bond failure, and ultimately fail due to fracture of the steel angles. Otherwise, significant bond slip occurs in the steel angles, and ultimately the columns fail due to the bond failure of steel angles or the fracture of transverse bars.
- Under cyclic lateral loading, the PSRC composite columns show about 20% lower deformation capacities than that of the conventional CES composite column. The lower deformation capacity of the PSRC composite columns is attributed to the following reasons: (1) relatively large plastic strains occur in the corner steel angles; (2) after spalling of the cover concrete, the exposed steel angles are susceptible to local buckling; and (3) the shear demand of the transverse reinforcement increases.
- In composite beam-PSRC composite column joints, the load-carrying capacity decreases because of the web local buckling of the U-section at the column face. Ultimately, the beam-column joints fail because of a tensile fracture of the buckled web plates initiated at the weld joint between the web and the bottom flange of the U-section. As yielding occurs in the web plate of the beam, significant web plate anchorage slip occurs inside the joint. However, the anchorage slip mitigates possible stress concentration that may be caused by the discontinuity of the flange plate, which contributes to the increase in deformation capacity.

Author details

Hyeon-Jong Hwang

Address all correspondence to: hwanggun85@naver.com

College of Civil Engineering, Hunan University, Changsha, Hunan, China

References

[1] Eom TS, Hwang HJ, Park HG, Lee CN, Kim HS. Flexural test for steel-concrete composite members using prefabricated steel angles. Journal of Structural Engineering. 2014;**140**(4): 04013094. DOI: 10.1061/(ASCE)ST.1943-541X.0000898

[2] Hwang HJ, Eom TS, Park HG, Lee SH, Kim HS. Cyclic loading test for beam-column connections of concrete-filled U-shaped steel beams and concrete-encased steel angle columns. Journal of Structural Engineering. 2015;**141**(11):04015020. DOI: 10.1061/(ASCE)ST.1943-541X.0001242

[3] Hwang HJ, Eom TS, Park HG, Lee SH. Axial load and cyclic lateral load tests for composite columns with steel angles. Journal of Structural Engineering. 2016;**142**(5):04016001. DOI: 10.1061/(ASCE)ST.1943-541X.0001452

[4] Kim HJ, Hwang HJ, Park HG, Kim DK, Yang JM. Eccentric axial load test of prefabricated composite columns using bolt-connected steel angles. Journal of Korean Society of Steel Construction. 2017;**29**(3):249-260. DOI: 10.7781/kjoss.2017.29.3.249

[5] Kim HJ, Hwang HJ, Park HG, Kim DK, Yang JM. Axial load test of prefabricated composite columns using bolt-connected steel angles. Journal of Korean Society of Steel Construction. 2017;**29**(2):147-158. DOI: 10.7781/kjoss.2017.29.2.147

[6] AWS (American Welding Society). Structural Welding Code-Reinforcing Steel (AWS D1.4). Miami; 1998. 45 p

[7] AWS (American Welding Society). Structural Welding Code-Steel (AWS D1.1). Miami; 2010. 540 p

[8] AISC (American Institute of Steel Construction). Specification for Structural Steel Building (ANSI/AISC 360-10). Chicago; 2010. 610 p

[9] Spacone E, El-Tawil S. Nonlinear analysis of steel-concrete composite structures: State of the art. Journal of Structural Engineering. 2004;**130**(2):159-168. DOI: 10.1061/(ASCE)0733-9445(2004)130:2(159)

[10] Hognestad E. A study of combined bending and axial load in reinforced concrete members. In: Bulletin Series. Vol. 399. Urbana, IL: Univ. of Illinois Engineering Experimental Station; 1951

[11] Mander JB, Priestley MJN, Park R. Theoretical stress strain model for confined concrete. Journal of Structural Engineering. 1988;**114**(8):1804-1826. DOI: 10.1061/(ASCE)0733-9445(1988)114:8(1804)

[12] Hoshikuma J, Kawashima K, Nagaya K, Taylor AW. Stress-strain model for confined reinforced concrete in bridge piers. Journal of Structural Engineering. 1997;**123**(5):624-633. DOI: 10.1061/(ASCE)0733-9445(1997)123:5(624)

[13] ACI (American Concrete Institute). Building Code Requirements for Structural Concrete and Commentary. ACI 318-14. Farmington Hills, MI; 2014. 520 p

[14] Eurocode 4. Design of Composite Steel and Concrete Structures-Part 1-1: General Rules and Rules for Buildings. Belgium: CEN; 2004. 122 p

IntechOpen

IntechOpen